DOI:10.1021/jf1031197

JOURNAL OF AGRICULTURAL AND FOOD CHEMISTRY
ARTICLE

Mass Spectral Analyses of Corn Stover Prehydrolysates To Assess Conditioning Processes

Richard F. Helm,*,† Judith Jervis,† W. Keith Ray,† Nicholas Willoughby,† Benjamin Irvin,† Jessica Hastie,† Daniel J. Schell,‡ and Nick Nagle‡

†Department of Biochemistry, Virginia Tech, Blacksburg, Virginia 24061-0910, United States, and ‡National Renewable Energy Laboratory, Golden, Colorado 80401, United States

Flow injection electrospray (FIE) and LC−tandem mass spectrometry techniques were used to characterize corn stover acid hydrolysates before and after overliming and ammonia conditioning steps. Analyses were performed on samples without fractionation (dilution only) in an effort provide an inventory of ionizable substances. Statistical evaluation of the results indicates that the ammonia-treated and crude hydrolysates were more similar to one another than any other pairing, with conditioning leading to a decrease in malate levels. LC−tandem mass spectrometry studies were also developed to characterize the oligosaccharides present in each hydrolysate utilizing a hydrophilic interaction chromatographic separation method. Neutral and acidic pentose-based oligosaccharides (xylodextrins) with degrees of polymerization between 2 and 5 were quantified with 4-*O*-methyl glucuronic acid-containing dimer and trimers predominating. Conditioning had little effect on the quantified oligosaccharide pool.

KEYWORDS: Conditioning; corn stover; malate; mass spectrometry; oligosaccharides; limit xylodextrins

INTRODUCTION

Agricultural biomass has re-emerged as a supplemental feedstock for liquid fuel (*1*). However, the conversion of lignified plant tissue into a flammable commodity chemical such as ethanol is technically challenging to perform efficiently at the industrial scale. Plant cell walls are not amenable to rapid degradation to fermentable sugars by microbial systems at a rate necessary for large-scale production schemes. Chemical pretreatments are therefore invoked (*2*) that depolymerize as well as degrade plant polymers, creating a complex array of degradation products (*3*−*5*), many of which are toxic to downstream bioprocessing schemes (*6*−*8*). While a general list of inhibitors including acetic acid, furans and phenolics is available (*7*, *9*, *10*), a complete understanding of quantitative changes and the potential synergistic effects of mixtures is not.

In order to increase the overall ethanol yield from chemically pretreated biomass, feedstocks are often detoxified, or "conditioned", to provide substrates that are more amenable to fermentation-based unit operations. The most common conditioning steps involve exposure to ammonia or lime (*3*, *5*, *8*). While efforts have been made to determine the mechanism(s) involved in the conditioning process (*11*), additional information on the conditioning mechanisms and the fate of biomass polymers during pretreatment processes is crucial to improving the efficiency of biomass-to-liquid fuel conversion schemes (*1*, *4*).

It is generally assumed that the detoxification process involves conversion or removal of toxic compounds derived from lignin (phenolic polymers) and carbohydrates (acetic acid and furans). However, clearly demonstrating this has been difficult for a number of reasons, with the lack of standards for lignin degradation products and higher oligosaccharides being one limiting factor. With the lack of standards, investigators generally monitor standard compounds through a detoxification step, assuming that the behavior of these compounds mirrors the behavior of all degradation products. To the best of our knowledge, the validity of such assumptions has never been tested experimentally. Alternative scenarios for dealing with the toxicity problem involve screening microbes in order to isolate strains capable of detoxifying furans and/or aromatic aldehydes, well-established inhibitors of ethanologens (*6*, *12*−*14*).

An approach to characterizing the hydrolysate pretreatment and conditioning steps that is unbiased with respect to standards availability has been lacking. Mass spectrometry coupled with statistical processing can potentially be used to first determine what compounds (as ions) are present in toxic and nontoxic hydrolysates based upon mass only (*15*−*17*). This would generate a list of ions that are modulated in their relative levels due to conditioning. Subsequent mass spectral fragmentation analysis of the key ions can then provide insight into the structures that are modified or reduced in level by the conditioning step. While LC−MS and GC−MS approaches have attempted to provide this insight, all analysis attempts to date have utilized an extraction step to isolate specific classes of compounds: generally those that are soluble in solvents such as ethyl acetate or methyl *tert*-butyl ether (*9*−*11*). Herein we describe our efforts to define the key ions present in untreated, overlimed and ammonia-treated corn stover hydrolysates. Flow injection electrospray mass spectrometry (FIE-MS) was used to provide profiles or mass spectral fingerprints for unconditioned and conditioned hydrolysates without prior fractionation. Subsequent studies evaluated the oligosaccharide pool in an effort to quantify changes in these materials due to the conditioning steps.

*Corresponding author. E-mail: helmrf@vt.edu. Fax: 540-231-4043.

 Published on Web 11/16/2010

MATERIALS AND METHODS

Materials. All organic solvents were LC−MS grade (Spectrum). Water was purified in-house (Milli-Q Biocel unit). Neutral xylooligosaccharide and 4-*O*-methyl glucuronoxylan oligosaccharide mixtures were obtained from Megazyme. Corn stover hydrolysates (crude, overlimed and ammonia-treated) were provided by the National Renewable Energy Laboratory (NREL). The corn stover was harvested from a farm in northeastern Colorado (Kramer Farm; Wray, CO), and reduced in size using a knife mill prior to pretreatment (*18*). Corn stover was treated with dilute sulfuric acid in a 900 dry kg/day pilot-scale continuous reactor operating at a solids concentration of 30% (w/w), and operating conditions of 190 °C, 0.048 g of acid/g of dry biomass, and an approximate residence time of 1 min (*19*). The pretreated slurry was compressed with a hydraulic press at 2000 psi that removed approximately 70% of the liquor from the pretreated solids. Overliming was performed as described previously (*20*). Ammonia-treated liquor was prepared by raising its pH to 8.5, holding at 30 °C for 30 min, and then lowering the pH to 6−7 with sulfuric acid. Both overliming and ammonia treatments resulted in a significant color change (darkening). A mock hydrolysate used for comparative purposes contained (in g/L): xylose, 80; glucose, 30; arabinose, 11; galactose, 7; cellobiose, 3; acetic acid, 12; and sulfuric acid, 12.

Flow Injection Electrospray Mass Spectrometry (FIE-MS). An API3200 triple quadrupole instrument (AB Sciex) was used in both positive and negative modes (100−800 *m*/*z*). Flow injection electrospray was conducted on samples diluted 5000-fold using a sample loop and autosampler (Agilent). Both the injection solvent and mobile phase were a 1:1 (v/v) mixture of MeOH:H_2O containing 0.1% formic acid (v/v). Flow rates were 25 μL/min with a run time of 10 min. Samples (20 μL) were injected randomly with 21 replicates for each hydrolysate (3 separate runs of 7 replicates each). A set of blanks and master mixes (1:1:1 mixture of each hydrolysate) was injected prior to the samples in order to establish a set of background ions. Analyses were performed initially in both the negative and positive ion modes, although final analyses were restricted to negative mode only. The mass spectrometer was operated at 170 °C with a voltage of −4.0 kV in negative mode and +4.5 kV in positive mode. The mass range evaluated was 100−800 *m*/*z*. Curtain gas was set to 10, and GS1 and GS2 gases were set to 35 and 55 (arbitrary units). The interface heater was used in all analyses, and declustering and entrance potentials were set to −24 and −5 in negative mode and +34 and +5 in positive mode. These values were set based upon maximizing signal intensity.

FIE-MS Data Analysis. Raw data was evaluated for integrity and feature (ion) ranking using the FIEmsPro workflow (*15*−*17*). As the analysis protocol and mass spectrometer used in this study were slightly different from that described in the original references, modification of the workflow used to process the data was required. Briefly, individual sample data sets were binned to 1 amu to generate matrices of sample vs *m*/*z*, with ion intensity at the intersection of each sample and *m*/*z* value. A scan range of 100−800 *m*/*z* thus provided 701 *m*/*z* ion intensities per sample. These matrices were subsequently processed through the FIEmsPro software to provide statistical analyses described in the text. The workflow and scripts used for data processing are provided in the Supporting Information.

Oligosaccharide Isolation and Analysis. Aliquots of the hydrolysates (6 mL) were neutralized to a pH between 5.5 and 5.9 with concentrated ammonium hydroxide. The resulting solution was passed through a precolumn of Bio-Gel P2 resin (2 g of resin rehydrated in water and flushed with at least 10 column volumes of water prior to use) in order to remove materials that bound to the P2 resin irreversibly. The flow-through containing carbohydrate was collected (8 mL) and added directly to a Bio-Gel P2 column (Bio-Rad; 2.5 cm × 250 cm, 72 g of resin) using water as the mobile phase (0.5 mL/min). Fractions (8 mL) were collected and analyzed individually by direct infusion mass spectrometry (negative ion mode). Dilutions ranged between 10 and 50 μL of the fraction diluted with a methanol:water (1 mL; 1:1, v/v) solution that contained 0.1% formic acid. Fractions with similar profiles were then combined and freeze-dried. Combined pools were further characterized by direct infusion mass spectrometry for structural confirmation and generation of multiple reaction monitoring conditions used for subsequent quantitative work. Anion-exchange chromatography with pulsed amperometric detection (HPAEC−PAD) was also performed to assess the oligosaccharide profiles and compare PAD and MS detection capabilities. Full details of the HPAEC−PAD methods can be found in the Supporting Information.

Structural characterization of the isolated oligosaccharides was performed utilizing tandem mass spectrometric analyses of the native and sodium borodeuteride-reduced oligosaccharides. The reduced oligosaccharides (alditols) were prepared by adding sodium borodeuteride (250 μL of a 150 mg/mL solution in 3 M aqueous ammonium hydroxide) to solutions of isolated oligosaccharides (3 mg in 300 μL of water). Excess reducing agent was quenched with glacial acetic acid, and the samples were frozen and subsequently concentrated to a solid on a high vacuum line equipped with a liquid nitrogen trap. The resulting alditols were desalted by passage through a gravity-fed P2 column using water as the eluent. Alditol-containing fractions were detected by spot testing on thin layer chromatography plates (aluminum-backed silica gel) using naphthoresorcinol staining. Samples were freeze-dried prior to mass spectral analysis.

HILIC−Tandem Mass Spectrometric Analysis of the Hydrolysates. Hydrolysates (1 mL) were diluted with water (4 mL) and adjusted to pH 5.7 with ammonium hydroxide at room temperature, cooled on ice for 30 min, and centrifuged to remove any particulates. The supernatants were collected and aliquots were diluted with 90% acetonitrile:10% 50 mM ammonium formate (pH 3.2) to provide between a 100- and 2000-fold dilution from the original hydrolysate. The HPLC separation utilized a binary LC unit (Agilent 1100 series with autosampler) and a minibore HILIC column (Kinetex 2.6 mm particles, 100 × 2.1 mm; Phenomenex) connected directly to an in-line filter (Krudkatcher Ultra; Phenomenex). The flow rate was maintained at 200 μL/min and sample injection volumes were 10 μL. Solvent A was 90% acetonitrile:10% 50 mM ammonium formate, pH 3.2 (v/v) and solvent B was acetonitrile:water:50 mM ammonium formate, pH 3.2 (50:40:10, v/v). The gradient regime began with 100% solvent A for 2 min followed by a 10 min linear ramp to 100% solvent B. The solvent ratio was held at 100% B for 7 min and returned to starting condition in 2 min, followed by an additional 16 min re-equilibration.

The mass spectrometer (AB Sciex 3200 triple quadrupole) was operated in the negative mode and employed multiple reaction monitoring for 21 ions utilizing parent and fragment ion pair conditions established with the oligosaccharides isolated above as well as neutral and acidic xylan oligosaccharide mixtures available commercially. A complete listing of mass spectral conditions can be found in the Supporting Information.

RESULTS AND DISCUSSION

The samples evaluated in this study were hydrolysates that resulted from the treatment of corn stover with hot aqueous sulfuric acid (*19*, *20*), with the crude hydrolysate defined as the aqueous material released from this treatment. Aliquots of this sample were conditioned by overliming (calcium hydroxide) as well as ammonia, providing three samples for comparison: crude, overlimed, and ammonia-pretreated. Initial flow injection electrospray (FIE) mass spectral analysis of negative and positive ion mode data sets indicated that the negative-ion mode provided significantly more ions. Hence, in-depth mass spectral and statistical analyses were restricted to the negative-ion mode.

A standard FIE-MS run consisted of two blank injections (solvent for hydrolysates; MeOH:H_2O), followed by 4 injections of a "master mix", or a solution composed of equal concentrations of each sample, and then random injection of the samples. The blank runs provided baseline instrument performance, the master mix a common background signal for the subsequent analyses, and the samples were randomized to minimize the effect of spectrometer performance. The three individual samples of corn stover hydrolysates (i.e., no true experimental replicates) were analyzed on three separate occasions (each on separate weeks) with 7 injections per sample. These data were combined to provide 21 mass spectral data sets per hydrolysate in the mass range of 100−800 *m*/*z* (mass-to-charge ratio). Each of the individual spectra are collected over the time range of elution and combined to generate a snapshot of the predominant ions present (**Figure 1**). It is important to note that this methodology does not effectively detect the dehydration products furfural ($[M - H]^-$, 95 amu; lower than mass range chosen) or HMF ($[M - H]^-$, 125 amu), as these substances do not ionize well in either positive or negative modes (*10*).

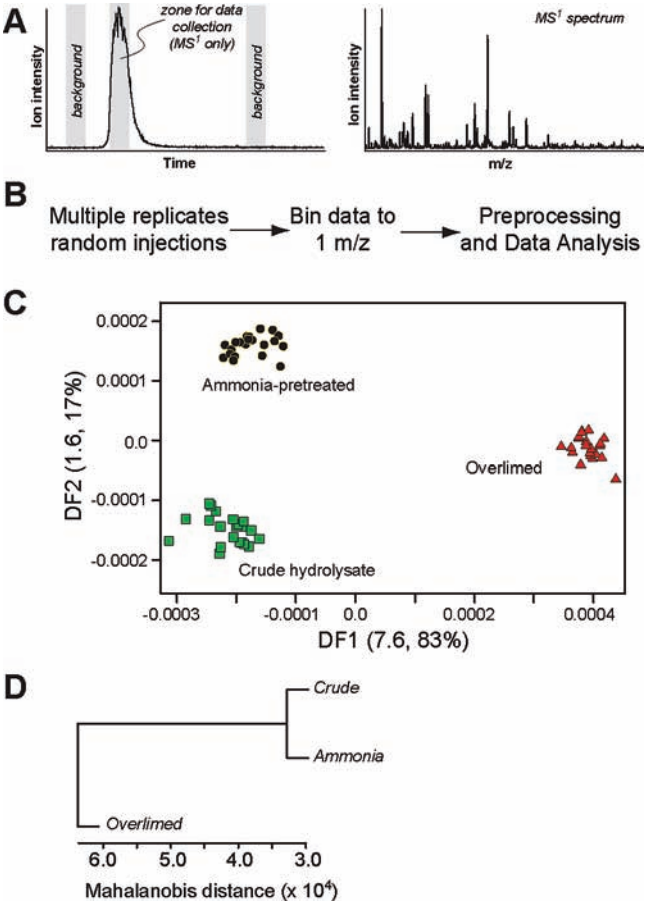

Figure 1. Graphical overview of the data analysis protocol and results. (**A**) Flow injection result displaying a peak for elution of the sample. Data are collected in MS^1-mode only (example spectrum on the right side of panel **A**) with scan obtained every second. Time windows before and after the peak are used for baseline subtraction. (**B**) The raw data for the individual analyses are binned to 1 amu resolution and subsequently processed and analyzed by the FIEmsPro tools (see Supporting Information for full program). (**C**) Multivariable analysis separates the individual samples into groups based upon the hydrolysates type. (**D**) The Mahalanobis distance is a measure of overall sample similarities.

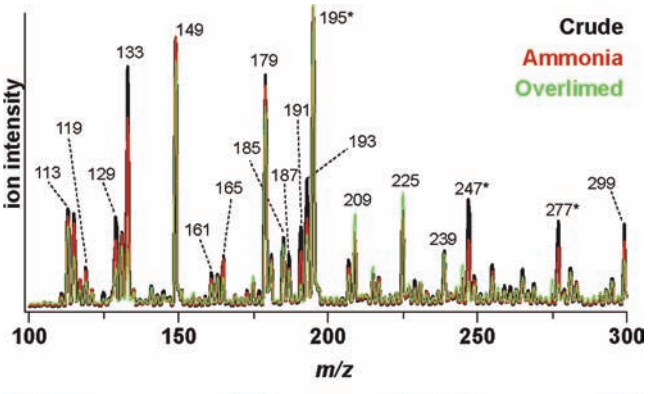

Compound	[M-H]⁻	Compound	[M-H]⁻
malonate	103	pentose	149
2-furoate	111	vanillin	151
maleate	115	di-OH-benzoate	153
fumarate	115	hydroxycoumarin	161
levulinate	115	*deoxyhexose*	*163*
methylmalonate	117	*p-coumarate*	*163*
succinate	117	vanillate	167
2-OH-2-methylbutyrate	117	gallate	169
4-OH-benzaldehyde	121	aconitate	173
benzoate	121	caffeate	179
5-OH-2-methylfurfural	125	hexose	179
itaconate	129	homovanillate	181
glutarate	131	syringaldehyde	181
malate	*133*	*citrate/isocitrate*	*191*
4-OH-acetophenone	135	*ferulate*	*193*
toluate	135	*hexuronate*	*193*
di-OH benzaldehyde	137	syringate	197
hydroxybenzoate	137	*methylglucuronate*	*207*
adipate	145	sinipinate	223

Figure 2. Averaged mass spectrum for the 100−300 *m/z* range. Ions at 149 and 179 are for pentose and hexose $[M - H]^-$, respectively. Ions assigned to cluster ions of sulfuric acid are indicated with an asterisk. Spectra are averages of 21 separate analysis performed on three separate occasions. The tabulated compound list provides the known hydrolysate constituents from previous studies. The compounds confirmed in this work are shown in italics.

Statistical Analysis Demonstrates That Each Hydrolysate Is Different. The FIE workflow permitted analysis of the data using several different statistical methods. The multivariable analysis shown in **Figure 1C** indicates that two discriminant functions (a linear combination of features that best separate the sample types) cleanly separate the samples into their respective sample classes. The Mahalanobis distance (**Figure 1D**) provides a visual representation of the statistical similarities between hydrolysates. The ammonia-treated sample has features similar to those of the crude hydrolysate, with the overlimed sample being the outlier. Features associated with the mass ranges of 100−300, 300−500 and 500−800 *m/z* are addressed separately below.

Analysis of the Mass Spectral Features: 100−300 *m/z*. The majority of mass spectral work associated with biomass pretreatment has concentrated on molecules with molecular weights less than 200 (*9*, *10*, *13*). As these previous studies utilized solvent: solvent extractions, the analyses were limited to molecules soluble in organic solvents. Whether or not there are substantial changes in more hydrophilic substances, and if these affect fermentation efficiencies is not known with certainty. The results in **Figure 2** indicate that, while there are changes in a few specific ions within this mass range, the overall number of ions that change dramatically in the 100−300 *m/z* window, as measured by flow injections, is relatively small, with *m/z* 133 clearly reduced in the overlimed sample.

The loss of three molecules of water from a pentose under acidic conditions leads to the formation of furfural. While the mechanism of this transformation has been investigated for decades (*21*−*23*), the exact process is still not fully understood. Recent computational studies suggest that the most favorable route energetically is via initial protonation of the *O*-2 hydroxyl, with subsequent dehydration (*23*). The loss of one molecule of water from a xylose would result in an expected *m/z* in the negative mode of 131, a process that can occur during the hydrolysis process as well as in the mass spectrometer. While a 131 ion was observed in the flow injection analysis of a mock hydrolysate (**Figure 3**), it was a minor contributor to the overall mass spectral profiles of all samples when compared to an ion at 133 *m/z*. Mass spectral fragmentation studies of this ion in comparison to standards with the same molecular weight led to the assignment of this ion as malic acid (**Figure 4A**). The water-soluble fraction of several different corn stover preparations was analyzed previously and found to contain between 1.6 and 5.7% malic acid by mass (*24*). Hence we can hypothesize that the malate is derived from the water-soluble component of corn stover.

Malate was not quantified in previous studies of corn stover prehydrolysates due to the use of an organic solvent extraction step (*10*). While malate (*S*-form) is an essential intermediate in the C4 carbon fixation pathway found in corn, is it an ethanologen inhibitor? Malic acid has been linked to low ethanol contents in

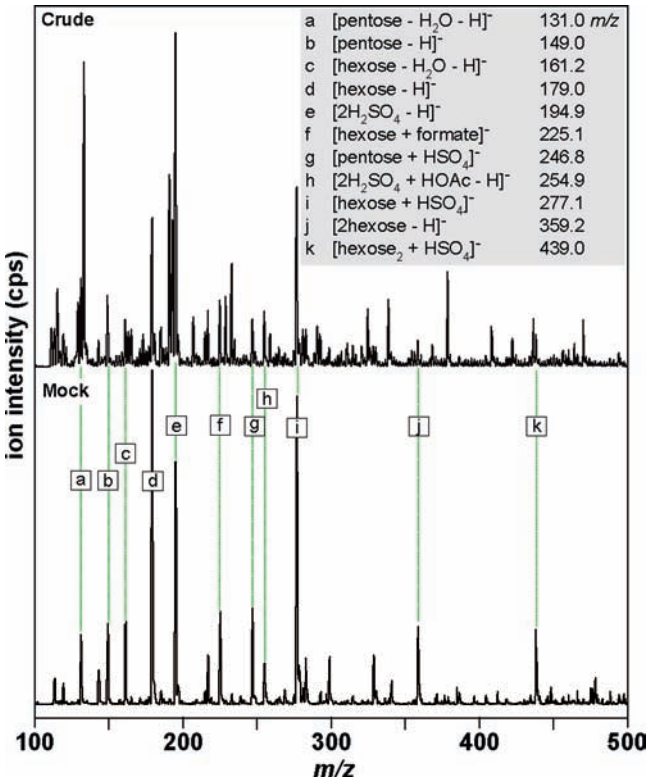

Figure 3. Mass spectral comparison of crude and mock hydrolysates. The mock hydrolysates contained (in g/L): xylose, 80; glucose, 30; arabinose, 11; galactose, 7; cellobiose, 3; acetic acid, 12; and sulfuric acid, 12. Key cluster ions are labeled and tabulated.

specific wines, with its presence requiring a deacidification step to increase ethanol levels (*25*). On the other hand, *S*-malate can be converted during fermentation processes to pyruvate, fumarate or oxaloacetate. The formation of pyruvate is an oxidative decarboxylation reaction performed by malic enzyme, which releases either NADH or NADPH. The formation of oxaloacetate by malate dehydrogenase is an oxidation reaction that yields reduced cofactor as well, whereas the formation of fumarate by fumarase is a nonoxidative dehydration reaction.

Toxins decrease ethanologen fermentation efficiencies, at least in part, by consuming reduced cofactor (NADH, NADPH) during detoxification, with the reduction of furfural to furfuryl alcohol (*12*, *26*, *27*) being an example. Microbial detoxification processes therefore generally decrease reduced cofactor supplies, whereas the conversions involving malate would increase reduced cofactor levels. While the toxicity of malate can be simply tested directly in model fermentation systems, it will also be necessary to determine the racemic composition of the hydrolysate-derived malate, as *R*-malate is a known inhibitor of the oxidative decarboxylating malic enzyme (*28*).

The cluster of ions at 191/193/195 also decreased in intensity after overliming and ammonia treatment (**Figure 2**). Based upon analysis of the fragmentation patterns for the individual standard compounds in comparison to the ion within the samples, the ion at 191 *m*/*z* was assigned as a mixture citrate and isocitrate (**Figure 4B**). Ion 193 is a combination of both ferulic and hexuronic acid as determined by comparison of the mass spectral fragmentation patterns of ferulic acid, galacturonic acid, glucuronic acid and the hydrolysate ion (**Figure 4C**). The 195 ion is predominantly a sulfuric acid cluster $[2H_2SO_4 - H]^-$ ion.

As the samples analyzed were submitted to a 5000-fold dilution step only, several of the ions identified in this mass range

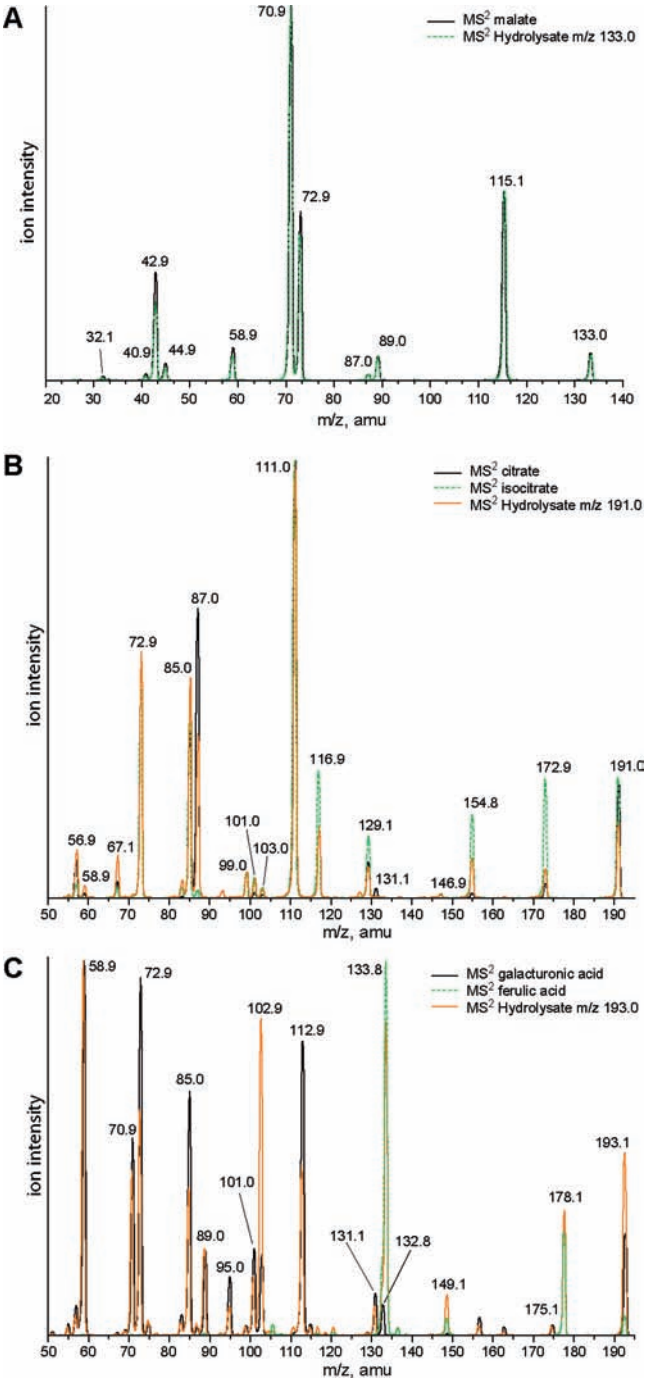

Figure 4. The mass spectral fragmentation patterns for malate (**A**), citrate/isocitrate (**B**), and ferulate/galacturonate (**C**) in comparison to hydrolysate-derived ions. The fragmentation pattern of glucuronate was indistinguishable from that of galacturonate and hence is not shown.

were complexes with hydrogen sulfate $[M + HSO_4^-]^-$, acetate $[M+OAc^-]^-$ and formate (**Figure 3**). Besides the 195 ion, ions at 209, 225, 247, 277, and 299 were analyzed by MS^2 and the fragmentation patterns matched that of [pentose + acetate]$^-$, [hexose + formate]$^-$, $[pentose + HSO_4^-]^-$, and $[hexose + HSO_4^-]^-$, and [2pentose − H]$^-$, respectively. The HSO_4^--containing adducts were readily identified by their characteristic/predominant 97 *m*/*z* ion in their negative ion mode tandem mass spectra whereas formate and acetate clusters exhibited [M − 46] and [M − 60], respectively. Decreases in the signal intensities for the sulfate adduct ions when comparing the crude and overlimed samples were presumably due to elimination of free sulfate via calcium sulfate precipitation during overliming.

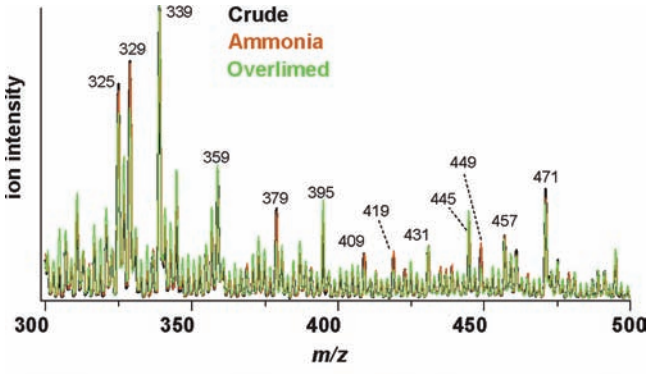

Compound	[M-H]	Compound	[M-H]
HexU-pentose	325	$Pent_2 + HSO_4^-$	379
$Pent_2$ + formate	327	Hex-Pent (?) + HSO_4^-	409
Hexose + pentose	329	HexU-$pent_2$	457
MeGlcU-pentose	339	MeGlcU-$pent_2$	471
2Hexose	359		

Figure 5. Averaged mass spectrum for the 300−500 *m*/*z* range. The tabulated compound list provides the ion identifications based upon mass spectral fragmentation and comparison to standards. Spectra are averages of 21 separate analysis performed on three separate occasions.

The decrease in adduct ions in the overlimed sample certainly contributed to the statistical placement of the overlimed sample apart from the crude and ammonia-treated samples (**Figure 1D**).

Analysis of the Mass Spectra Features: 300−500 *m*/*z*. Ionizable compounds in this mass region were anticipated to be composed of lignin and polysaccharide oligomers. As lignin is a complex biopolymer prone to acid-catalyzed depolymerization and degradation, a complex array of compounds will be formed. **Figure 5** indicates that there is an overall increase in signal intensity for almost all ions in going from crude to ammonia-treated and overlimed hydrolysates, opposite of that observed for the lower mass range. This is presumably due to the conditioning chemistry, which leads to an array of compounds with similar molecular weights. The most striking features in this mass range were the intensities of the uronosyl-pentose-containing dimers (*m*/*z* 325, 339) and trimers (*m*/*z* 457, 471). Based upon mass spectral fragmentation patterns and comparison with standards, the 339/471 pair contains a 4-*O*-methylglucuronic acid moiety while the 325/457 ion series is derived from a non-methylated hexuronic acid (**Figure 6**). Considering the known pentosans in corn stover and the lability of an L-arabinofuranosyl bond, it is assumed that these dimers and trimers contain xylose as the core pentose.

Several of the predominant ions were evaluated by mass spectral fragmentation analysis, and the results are tabulated in **Figure 5**. While a 329 ion was the most predominant ion observed in the negative mode mass spectral analysis of acid-extracted wheat straw lignin and assigned to a phenylcoumaran-type dimer (*29*), this ion in our samples was a cluster ion of a pentose and hexose, $[\text{pentose} + \text{hexose} - \text{H}]^-$. Recent efforts in lignin oligomer mass spectral sequencing described model compound fragmentation data (negative mode) for compounds with masses similar to those found here (*30*). However, none of the ions reported herein had fragmentation patterns similar to those reported in the lignin sequencing work. The ion at *m*/*z* 409 was assigned to a $[\text{hexose} - \text{pentose} + \text{HSO}_4]^-$ dimer. Fragmentation analysis of the corresponding $[\text{hexose} - \text{pentose} - \text{H}]^-$ ion (311 *m*/*z*) revealed ions for both the intact and dehydrated pentose and hexose moieties as well as cross-ring cleavages (A- or X-type cleavages) (*31*). It was not possible however to discern the reducing end carbohydrate(s) or the linkage position(s). Whether this molecule is a natural constituent of noncellulosic polysaccharides in corn stover or a reversion product (*32*, *33*) is presently not known.

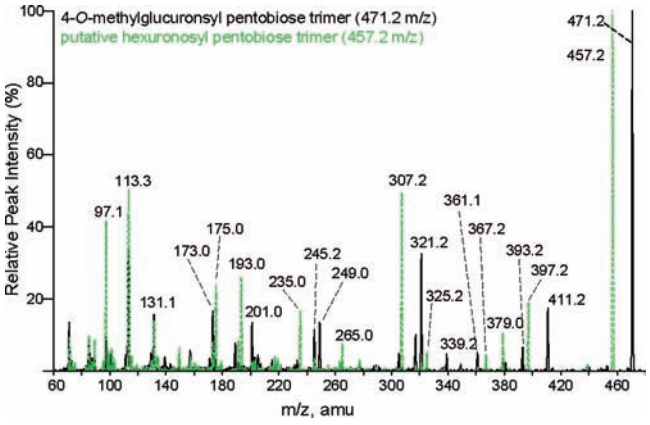

Figure 6. MS^2 spectra of methyated (471.2 *m*/*z*) and unmethylated (457.2 *m*/*z*) uronosyl-containing trisaccharides.

Analysis of the Mass Spectra Features: 500−800 *m*/*z*. Relatively few ions predominated in the averaged mass spectra within this mass range (see Supporting Information), with a decrease in discernible ions as one moves from the crude to ammonia-treated and subsequently overlimed samples. Statistical analyses indicated that several ions were different, including 505, 531, 599, and 629 *m*/*z*. These ions may be derived from lignin (*29*, *30*, *34*, *35*) as they do not match known oligosaccharide structures; confirmation is the subject of ongoing investigations.

Corn Stover Acid Hydrolysis Yields "Limit Xylodextrins". Improved conversion of biomass to ethanol will require the efficient release of all polysaccharides to free sugar. The flow injection analyses of the hydrolysates reported here indicated that a significant pool of oligosaccharides are present, and thus efforts were undertaken to isolate and characterize this pool of compounds. Neutralization of the hydrolysates followed by size exclusion chromatography provided an oligosaccharide-enriched sample that was analyzed by direct infusion mass spectrometry as well as LC−MS/MS. Direct infusion mass spectrometry confirmed the presence of the oligosaccharides with a maximum degree of polymerization of 12. Structures were confirmed by mass spectral fragmentation analyses of both the native and sodium borodeuteride-reduced oligomers. The vast majority of these oligomers contained one 4-*O*-methylglucuronic acid or hexuronic acid residues (**Table 1**). The native oligosaccharides from the three hydrolysates studied were devoid of quantifiable levels of acetyl-containing oligosaccharides although such oligosaccharides could be detected when nonreduced samples were fractionated by size exclusion chromatography and subsequently analyzed by mass spectrometry. There were also a series of higher saccharides that contained two uronosyl moieties, and neutral pentose-based oligosaccharides with between 1 and 3 acetate groups. Based upon ion intensities from the direct infusion analysis of the purified oligosaccharides, there were significantly less non-methylated hexuronic acids present in the hydrolysates than the methylated variants. Dimers through pentamers were the predominant oligosaccharides present, materials we term "limit xylodextrins".

Oligosaccharide Separation and Quantification Can Be Performed by Hydrophilic Interaction Chromatography−Tandem Mass Spectrometry. Due to the structure of noncellulosic polysaccharides, there are multiple structures that can provide the same oligosaccharide ion. For example, a xylodextrin composed of three xyloses and one uronic acid has three different possible isomers: the uronic acid can be attached at the reducing, middle, and/or nonreducing xylose moiety (*36*). No information is presently available on the complexity of corn stover-derived isobaric oligosaccharide pools or if conditioning modulates oligosaccharide profiles. In an effort

Table 1. Oligosaccharides Confirmed by Tandem Mass Spectrometry To Be Present in Corn Stover Prehydrolysates[a]

oligosaccharide	$[M - H^+]^-$	acetates
$(pentose)_2$	281.1	0, 1
$(pentose)_3$	413.1	0, 1
$(pentose)_4$	545.2	0, 1, 2
$(pentose)_5$	677.2	0, 1, 2, 3
hexose-pentose	311.1	0
$(hexose)_2$	341.1	0
$(hexose)_3$	503.2	0
$(hexose)_4$	665.2	0
uronosyl-(pent)	325.1	0
4-*O*-Me-Uronosyl-(pent)	339.1	0
uronosyl-$(pent)_2$	457.1	0
4-*O*-Me-uronosyl-$(pent)_2$	471.1	0
uronosyl-$(pent)_3$	589.2	0, 1
4-*O*-Me-uronosyl-$(pent)_3$	603.2	0, 1
uronosyl-$(pent)_4$	721.2	0, 1, 2
4-*O*-Me-uronosyl-$(pent)_4$	735.2	0
4-*O*-Me-uronosyl-$(pent)_5$	867.2	0
4-*O*-Me-uronosyl-$(pent)_6$	999.3	0
4-*O*-Me-uronosyl-$(pent)_7$	1131.4	0, 1
4-*O*-Me-uronosyl-$(pent)_8$	1263.4	0, 1
4-*O*-Me-uronosyl-$(pent)_9$	1395.4	0
4-*O*-Me-uronosyl-$(pent)_{10}$	1527.5	0
4-*O*-Me-uronosyl-$(pent)_{11}$	1659.5	0
(4-*O*-Me-uronosyl)2-$(pent)_7$	1322.4	0
(4-*O*-Me-uronosyl)2-$(pent)_8$	1454.5	0
(4-*O*-Me-uronosyl)2-$(pent)_9$	1586.5	0
(4-*O*-Me-uronosyl)2-$(pent)_{10}$	1718.5	0
(4-*O*-Me-uronosyl)2-$(pent)_{11}$	1850.6	0

[a] $[M - H]^-$ is the mass value for the unacetylated oligosaccharide. Each acetate adds an additional 42 Da. Several higher mass oligosaccharides were also present as $[M - 2H^+]^{-2}$ ions.

to quantify the oligosaccharides present in the three corn stover hydrolysates, a HILIC-based fractionation and multiple reaction monitoring (MRM) mass spectrometry protocol was developed for several of the predominant oligomers. The native oligosaccharides isolated by size exclusion chromatography as well as commercially available xylan-based oligomers were used to develop the MRM detection parameters via direct infusion. With these parameters in place, a HILIC-based separation protocol was optimized to separate and quantify the oligosaccharides present in the three hydrolysates. Sample preparation involved neutralization of each sample to pH 5.7, dilution into 90:10 acetonitrile:50 mM ammonium formate (pH 3.2) and injection. A gradient to higher ammonium formate provided separation and quantification of the oligomers as shown in **Figure 7A**.

HILIC-based chromatographic separations rely primarily upon partitioning of analytes between a water-enriched layer of solvent near the solid phase surface and the bulk solvent. Analytes will partition into the layer based upon their relative solubilities combined with their ability to hydrogen bond and ion-exchange with the solid phase surface. In the case of corn stover oligosaccharides, the smaller neutral pentose-based oligomers eluted first with the acidic oligosaccharides eluting later in the gradient (**Figure 7A**). Neutral hexose-based oligomers eluted slightly later than their corresponding pentose oligomers. The main limitation of the method is the solubility of the oligosaccharides in the mobile phase at the start of the gradient: 90:10 acetonitrile:50 mM ammonium formate. Injecting materials at concentrations of aqueous buffer higher than the initial concentration in the mobile phase, a condition that would ensure solubilization of the higher oligosaccharides (degrees of polymerization greater than 6), led to poor separations of the lower molecular weight oligomers (dimers predominantly). This was presumed to be due to modification of

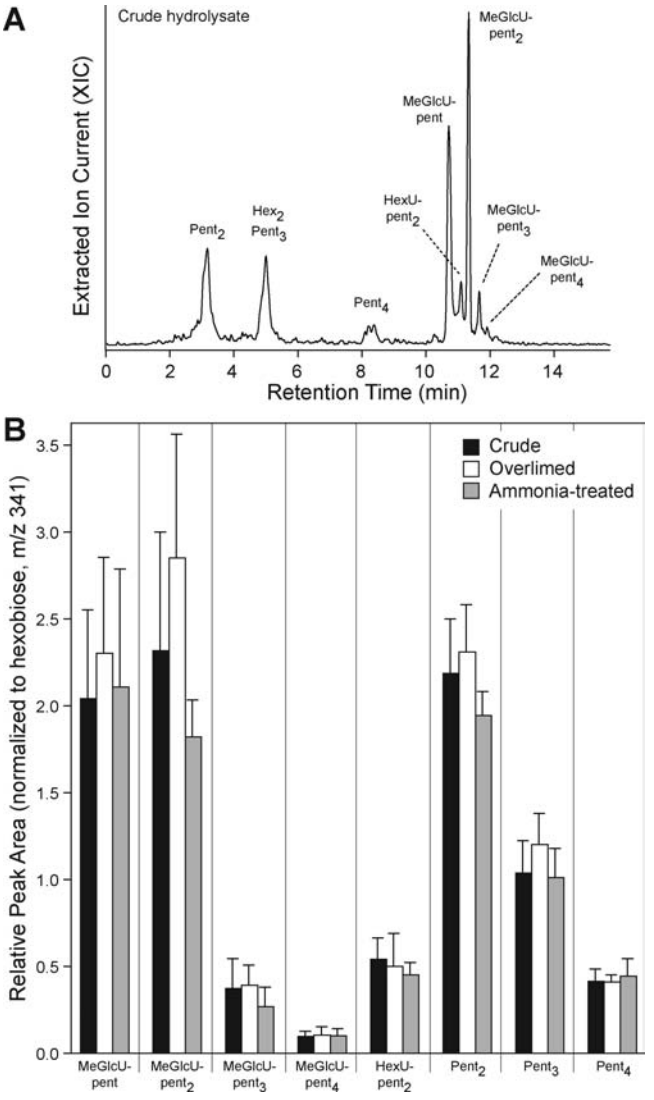

Figure 7. HILIC-based separation and MRM-based quantification of selected oligosaccharides. The chromatogram (**A**) displays the separation characteristics of the system (summed ion current for the 21 oligosaccharides quantified). The bar graph (**B**) displays the quantitative data for several different oligosaccharides. The analyses were performed in triplicate.

the aqueous layer at the surface of the column packing material. As we were interested in determining the relative levels of pentose- and hexose-based dimers, we focused our attention on oligosaccharides with degrees of polymerization less than five.

Oligosaccharide Levels Are Unaffected by Overliming and Ammonia Treatments. The levels of oligosaccharides present in crude, overlimed, and ammonia-treated hydrolysates are shown in **Figure 7B**. These data were normalized to the hexobiose peak, which was found to remain constant in these samples. There was no significant difference in oligosaccharide levels between samples, indicating that conditioning steps involving overliming and ammonia treatment have little effect on the oligosaccharide pool. There may be decreases in acetylated oligosaccharides, but the samples investigated here were low in these substances to begin with. The level of oligomers present in solution will be a balance between acid hydrolysis kinetics (reaction parameters) and solubility. Upon cooling of hydrolysis mixtures, solubilized corn stover oligosaccharides may redeposit into the solids fraction, either free or associated with lignin (*37*). Long-term storage of prehydrolysates will result in the formation of a precipitate, supporting the concept

that redeposition is a factor that must be considered when improving overall conversion efficiency. While this is suggestive of lignin−carbohydrate complexes, no mass spectral evidence was obtained for such structures in this work. As hydrolysates are concentrated mixtures, phenol−carbohydrate interactions may be both covalent and noncovalent, and highly dependent on temperature and pH.

SUMMARY AND IMPLICATIONS FOR FURTHER WORK

Flow injection electrospray (FIE) mass spectrometry with statistical data processing was used to evaluate the compounds present in corn stover hydrolysates before and after two different conditioning regimes. While similar studies have been performed in the past, this work analyzed samples that had not been fractionated or derivatized in an effort to provide an unbiased "systems-level" survey of the prehydrolysate. FIE analysis of an individual sample is complete in 10 min, and with an autosampler, the protocol is quite amenable to multiple unattended runs. Subsequent data analysis using the pre-established pipeline (*15*−*17*) and with multiple replicates provides an overview of sample differences. Such methodologies, especially when combined with targeted ion monitoring, should prove useful for the comparison of treatment regimes and/or clonal crops for improved conversion efficiencies.

While the FIE analyses have provided a glimpse into the full complexity of prehydrolysate liquors, the method is not without limitations. The presence of sulfuric acid in the diluted samples provides cluster ions that can change dramatically in signal intensity, especially when comparing crude and overlimed samples. This difference in sulfuric acid levels clearly contributed to the statistical clustering results (**Figure 1C**,**D**), which indicated that the overlimed sample was the "outlier". The presence of both lignin and carbohydrate components provides an unknown degree of ion suppression, while also potentially making compound identification difficult. There are several phenolic- and carbohydrate-derived compounds expected to be present in the hydrolysates whose exact masses cannot be differentiated by the instrument used in this study, two examples being ferulic/hexuronic acids (m/z 193) and *p*-coumaric acid/deoxyhexoses (m/z 163). Differentiating phenolic- and carbohydrate-derived ion series based upon mass only is complicated by the fact that lignin methoxyl content (*p*-hydroxyphenyl vs guaiacyl vs syringyl; 30 Da mass difference) is the same mass change for a pentose to a hexose. In the case of ferulic acid and hexuronic acids, differentiation was made possible by their corresponding fragmentation patterns and the availability of standards. Such is not the case for many higher molecular weight compounds.

Nonetheless, we have shown that the organic acids malate, citrate, and isocitrate are present in corn stover hydrolysates, with these acids decreasing in concentration upon conditioning (**Figure 4A**,**B**). Prehydrolysate liquors also contain significant levels of higher molecular weight (200−800 m/z) materials including xylan and lignin oligomers. Sulfuric acid-based cluster ions are factors in FIE analysis of hydrolysates. Thus when considering future FIE-based analyses, sulfate removal followed by a solid phase extraction protocol (to separate the polar and nonpolar species) should be explored.

Statistical analysis of the raw data supports the concept that overliming and ammonia treatments provide different molecular pools. While both show reductions in malate, the ammonia-treated sample is more similar to the crude hydrolysate than the overlimed, which is partly due to sulfuric acid levels in the hydrolysates (crude > ammonia > overlimed). While one of our initial goals was to identify conditioning mechanisms through the ranking of key ions, this is problematic due to the complex nature of the individual hydrolysates. Fractionation as described above should lead to a better overall understanding of hydrolysate conditioning chemistry.

An important outcome of the efforts described here is the establishment of relatively simple methods for carbohydrate oligomer enrichment and analysis. Uronosyl-containing and neutral pentosans are present in significant and quantifiable levels, with the lower molecular weight oligomers unaffected by conditioning. To our knowledge, this is the first documentation of non-methylated hexuronic acid-containing oligomers in corn stover hydrolysates. As work that attempts to release the xylose bound within these limit xylodextrins will dramatically improve ethanol fermentation efficiencies, application of the protocols described here will permit a quantitative assessment of oligomer levels during hydrolysate production, as well as their fates during subsequent conditioning and fermentation processes.

There are also fundamental applications for the methodologies described. In-depth analysis of the purified oligosaccharides revealed a series of oligomers with two 4-*O*-methyl uronosyl side chains as well as neutral pentosans with up to three acetate groups (**Table 1**). These xylan substructures suggest that limited and controlled hydrolysis studies combined with LC−tandem mass spectrometry can provide insight into overall heteropolysaccharide structure, similar to what has been accomplished enzymatically (*38*, *39*). For example, in our investigations, we observed a decrease in ion abundances for the diuronosyl substructures when the core pentosan chain becomes less than eight units long. Quantitative assessment of the distribution of uronosyl residues over xylan chains is therefore quite feasible using mass spectrometry. Confirmation of the hexose-pentose dimer (m/z 409; **Figure 5**) as well as the fate of non-xylan polysaccharides such as mixed linkage glucans and pectin should also be possible. Chemotypic assessment of cultivars as well as genetically modified lines by mass spectrometry can lead to an understanding of heteropolysaccharide biosynthetic processes. In addition, the combination of chemotypic and fermentation efficiency data will lead to the rapid isolation of lines that are the most amenable to biofuel conversion.

ACKNOWLEDGMENT

We thank Dr. Manfred Beckmann (Institute of Biological Sciences, Aberystwyth University) for several helpful conversations and R-based scripting. We also acknowledge Dr. Roderick V. Jensen (Department of Biological Sciences, Virginia Tech) for his help in scripting, and Edward Jennings (NREL) for his work in preparing the hydrolysate samples.

Supporting Information Available: Full details of HPAEC−PAD methods, workflow and scripts used for data processing, and complete listing of mass spectral conditions. This material is available free of charge via the Internet at http://pubs.acs.org.

LITERATURE CITED

(1) Lynd, L. R.; Laser, M. S.; Bransby, D.; Dale, B. E.; Davison, B.; Hamilton, R.; Himmel, M.; Keller, M.; McMillan, J. D.; Sheehan, J.; Wyman, C. E. How biotech can transform biofuels. *Nat. Biotechnol.* **2008**, *26* (2), 169−72.

(2) Himmel, M. E. *Biomass recalcitrance: Deconstructing the plant cell wall for bioenergy*; Blackwell Pub.: Oxford, 2008.

(3) Alriksson, B.; Sjode, A.; Nilvebrant, N. O.; Jonsson, L. J. Optimal conditions for alkaline detoxification of dilute-acid lignocellulose hydrolysates. *Appl. Biochem. Biotechnol.* **2006**, *130* (1−3), 599−611.

(4) Himmel, M. E.; Bayer, E. A. Lignocellulose conversion to biofuels: current challenges, global perspectives. *Curr. Opin. Biotechnol.* **2009**, *20* (3), 316−7.

(5) Pienkos, P. T.; Zhang, M. Role of pretreatment and conditioning processes on toxicity of lignocellulosic biomass hydrolysates. *Cellulose* **2009**, *16* (4), 743−62.
(6) Almeida, J. R. M.; Bertilsson, M.; Gorwa-Grauslund, M. F.; Gorsich, S.; Liden, G. Metabolic effects of furaldehydes and impacts on biotechnological processes. *Appl. Microbiol. Biotechnol.* **2009**, *82* (4), 625−38.
(7) Klinke, H. B.; Thomsen, A. B.; Ahring, B. K. Inhibition of ethanol-producing yeast and bacteria by degradation products produced during pre-treatment of biomass. *Appl. Microbiol. Biotechnol.* **2004**, *66* (1), 10−26.
(8) Nilvebrant, N. O.; Persson, P.; Reimann, A.; De Sousa, F.; Gorton, L.; Jonsson, L. J. Limits for alkaline detoxification of dilute-acid lignocellulose hydrolysates. *Appl. Biochem. Biotechnol.* **2003**, *105* −*108*, 615−28.
(9) Persson, P.; Andersson, J.; Gorton, L.; Larsson, S.; Nilvebrant, N. O.; Jonsson, L. J. Effect of different forms of alkali treatment on specific fermentation inhibitors and on the fermentability of lignocellulose hydrolysates for production of fuel ethanol. *J. Agric. Food Chem.* **2002**, *50* (19), 5318−25.
(10) Sharma, L. N.; Becker, C.; Chambliss, C. K. Analytical characterization of fermentation inhibitors in biomass pretreatment samples using liquid chromatography, UV-visible spectroscopy, and tandem mass spectrometry. *Methods Mol. Biol.* **2009**, *581*, 125−43.
(11) Ranatunga, T. D.; Jervis, J.; Helm, R. F.; McMillan, J. D.; Wooley, R. J. The effect of overliming on the toxicity of dilute acid pretreated lignocellulosics: the role of inorganics, uronic acids and ether-soluble organics. *Enzyme Microb. Technol.* **2000**, *27* (3−5), 240−7.
(12) Heer, D.; Heine, D.; Sauer, U. Resistance of Saccharomyces cerevisiae to High Concentrations of Furfural Is Based on NADPH-Dependent Reduction by at Least Two Oxireductases. *Appl. Environ. Microbiol.* **2009**, *75* (24), 7631−8.
(13) Heer, D.; Sauer, U. Identification of furfural as a key toxin in lignocellulosic hydrolysates and evolution of a tolerant yeast strain. *Microb. Biotechnol.* **2008**, *1*, 497−506.
(14) Nichols, N. N.; Sharma, L. N.; Mowery, R. A.; Chambliss, C. K.; van Walsum, G. P.; Dien, B. S.; Iten, L. B. Fungal metabolism of fermentation inhibitors present in corn stover dilute acid hydrolysate. *Enzyme Microb. Technol.* **2008**, *42* (7), 624−30.
(15) Beckmann, M.; Parker, D.; Enot, D. P.; Duval, E.; Draper, J. High-throughput, nontargeted metabolite fingerprinting using nominal mass flow injection electrospray mass spectrometry. *Nat. Protoc.* **2008**, *3* (3), 486−504.
(16) Enot, D. Preprocessing, classification modeling and feature selection using flow injection electrospray mass spectrometry metabolite fingerprint data. *Nat. Protoc.* **2008**, *3*, 446−70.
(17) Overy, D. P. Explanatory signal interpretation and metabolite identification strategies for nominal mass FIE-MS metabolite fingerprints. *Nat. Protoc.* **2008**, *3*, 471−85.
(18) Weiss, N. D.; Farmer, J. D.; Schell, D. J. Impact of corn stover composition on hemicellulose conversion during dilute acid pretreatment and enzymatic cellulose digestibility of the pretreated solids. *Bioresour. Technol.* **2010**, *101* (2), 674−8.
(19) Schell, D. J.; Farmer, J.; Newman, M.; McMillan, J. D. Dilute-sulfuric acid pretreatment of corn stover in pilot-scale reactor: investigation of yields, kinetics, and enzymatic digestibilities of solids. *Appl. Biochem. Biotechnol.* **2003**, *105* −*108*, 69−85.
(20) Mohagheghi, A.; Ruth, M.; Schell, D. J. Conditioning hemicellulose hydrolysates for fermentation: Effects of overliming pH on sugar and ethanol yields. *Process Biochem.* **2006**, *41* (8), 1806−11.
(21) Antal, M. J.; Leesomboon, T.; Mok, W. S.; Richards, G. N. Mechanism of formation of 2-furaldehyde from image-xylose. *Carbohydr. Res.* **1991**, *217*, 71−85.
(22) Feather, M. S.; Harris, D. W.; Nichols, S. B. Routes of conversion of D-xylose, hexuronic acids, and L-ascorbic acid to 2-furaldehyde. *J. Org. Chem.* **1972**, *37*, 1606−8.
(23) Nimlos, M. R.; Qian, X.; Davis, M.; Himmel, M. E.; Johnson, D. K. Energetics of Xylose Decomposition as Determined Using Quantum Mechanics Modeling. *J. Phys. Chem. A* **2006**, *110* (42), 11824−38.
(24) Chen, S. F.; Mowery, R. A.; Scarlata, C. J.; Chambliss, C. K. Compositional analysis of water-soluble materials in corn stover. *J. Agric. Food Chem.* **2007**, *55* (15), 5912−8.
(25) Sousa, M. J.; Mota, M.; Leao, C. Effects of ethanol and acetic acid on the transport of malic acid and glucose in the yeast Schizosaccharomyces pombe: implications in wine deacidification. *FEMS Microbiol. Lett.* **1995**, *126* (2), 197−202.
(26) Lin, F. M.; Tan, Y.; Yuan, Y. J. Temporal quantitative proteomics of Saccharomyces cerevisiae in response to a nonlethal concentration of furfural. *Proteomics* **2009**, *9* (24), 5471−83.
(27) Lin, F. M.; Qiao, B.; Yuan, Y. J. Comparative proteomic analysis of tolerance and adaptation of ethanologenic Saccharomyces cerevisiae to furfural, a lignocellulosic inhibitory compound. *Appl. Environ. Microbiol.* **2009**, *75* (11), 3765−76.
(28) Yamaguchi, M.; Tokushige, M.; Katsuki, H. Studies on regulatory functions of malic enzymes. II. Purification and molecular properties of nicotinamide adenine dinucleotide-linked malic enzyme from Eschericha coli. *J. Biochem.* **1973**, *73*, 169−80.
(29) Banoub, J. H.; Benjelloun-Mlayah, B.; Ziarelli, F.; Joly, N.; Delmas, M. Elucidation of the complex molecular structure of wheat straw lignin polymer by atmospheric pressure photoionization quadrupole time-of-flight tandem mass spectrometry. *Rapid Commun. Mass Spectrom.* **2007**, *21* (17), 2867−88.
(30) Morreel, K.; Dima, O.; Kim, H.; Lu, F.; Niculaes, C.; Vanholme, R.; Dauwe, R.; Goeminne, G.; Inzé, D.; Messens, E.; Ralph, J.; Boerjan, W. Mass spectrometry-based sequencing of lignin oligomers. *Plant Physiol.* **2010**, *153*, 1464−78.
(31) Domon, B.; Costello, C. E. A systematic nomenclature for carbohydrate fragmentations in FAB-MS/MS spectra of glycoconjugates. *Glyconjugate J.* **1988**, *5*, 397−409.
(32) Pilath, H.; Nimlos, M.; Mittal, A.; Himmel, M.; Johnson, D. Glucose reversion reaction kinetics. *J. Agric. Food Chem.* **2010**, *58* (10), 6131−40.
(33) Helm, R. F.; Young, R. A.; Conner, A. H. Reversion reactions of D-glucose during the hydrolysis fo cellulose with dilute sulfuric acid. *Carbohydr. Res.* **1989**, *185*, 249−60.
(34) Banoub, J. H.; Delmas, M. Structural elucidation of the wheat straw lignin polymer by atmospheric pressure chemical ionization tandem mass spectrometry and matrix-assisted laser desorption/ionization time-of-flight mass spectrometry. *J. Mass Spectrom.* **2003**, *38* (8), 900−3.
(35) Evtuguin, D. V.; Amado, F. M. L. Application of Electrospray ionization mass spectrometry to the elucidation of the primary structure of lignin. *Macromol. Biosci.* **2003**, *3* (7), 339−43.
(36) Naran, R.; Black, S.; Decker, S. R.; Azadi, P. Extraction and characterization of native heteroxylans from delignified corn stover and aspen. *Cellulose* **2009**, *16*, 661−75.
(37) Brunecky, R.; Vinzant, T. B.; Porter, S. E.; Donohoe, B. S.; Johnson, D. K.; Himmel, M. E. Redistribution of xylan in maize cell walls during dilute acid pretreatment. *Biotechnol. Bioeng.* **2009**, *102* (6), 1537−43.
(38) Puchart, V.; Biely, P. Simultaneous production of endo-beta-1,4-xylanase and branched xylooligosaccharides by Thermomyces lanuginosus. *J. Biotechnol.* **2008**, *137* (1−4), 34−43.
(39) Togashi, H.; Kato, A.; Shimizu, K. Enzymatically derived aldouronic acids from Eucalyptus globulus glucuronoxylan. *Carbohydr. Polym.* **2009**, *78* (2), 247−52.

Received for review August 11, 2010. Revised manuscript received November 4, 2010. Accepted November 5, 2010. This work was funded by the Biomass Program of the US Department of Energy through NREL Subcontract NDJ-7-77600 to Virginia Tech.